Eur Biophys J (2003) 31: 595–607
DOI 10.1007/s00249-002-0255-x

ARTICLE

**Niklas Engler · Valeri Prusakov · Andreas Ostermann**
**Fritz G. Parak**

# A water network within a protein: temperature-dependent water ligation in H64V-metmyoglobin and relaxation to deoxymyoglobin

Received: 11 July 2002 / Accepted: 30 August 2002 / Published online: 1 November 2002


**Abstract** The sperm whale myoglobin mutant H64V, where the distal histidine is mutated to valine, is known to be five coordinated in the ferric state at room temperature and physiological pH. A change of the ligation in this H64V-Mbmet has been observed by optical absorption spectroscopy as a function of temperature from 20 K to 300 K. Above the dynamical transition at about 180 K one observes the temperature-dependent equilibrium between five- and six-ligated heme. Below the dynamical transition the equilibrium is frozen-in at about 50% of six-coordinate molecules. The water ligation of the iron occurs at temperatures where protein-specific motions are present, as monitored by Mössbauer spectroscopy. The X-ray structures of H64V-Mbmet at 300 K and 110 K are reported with a resolution of 1.5 Å and 1.3 Å, respectively. The measurements at high resolutions are possible owing to crystallization in the space group $P2_1$, whereas all mutant myoglobins studies up to now have been carried out with crystals in the space group *P*6. The overall structure at both temperatures is very close to the native myoglobin. The binding of water at the sixth coordination site at lower temperatures is possible owing to a stabilizing water network extending from the protein surface to the active centre. The reduction of the H64V-Mbmet by electrons obtained by X-ray irradiation of the water-glycerol solvent at 85 K produces an intermediate low-spin state of the water-ligated molecules where Fe(II) retains the six-fold coordination. Mössbauer spectroscopy shows that the relaxation of the metastable low-spin state to high-spin H64V-Mbdeoxy with dissociation of the Fe(II)-$H_2O$ bond starts at about 115 K and is completed at about 170 K. Differences in the dynamics properties of the native and mutant myoglobin and the connection to the dynamical transition around 180 K are discussed.

**Keywords** Heme protein · X-ray structure analysis · Dynamical transition · Protein dynamics · Intermediate state

N. Engler · A. Ostermann · F.G. Parak (✉)
Physik-Department E17,
Technische Universität München, 85747 Garching, Germany
E-mail: fritz.parak@ph.tum.de
Tel.: +49-89-28912551
Fax: +49-89-28912548

V. Prusakov
Institute of Chemical Physics,
RAS, 117334 Moscow, Russia

## Introduction

Mammalian myoglobin (Mb) reversibly binds molecular oxygen and provides its storage and release in the muscles. Recent investigations suggest that it is also involved in the NO-related chemistry of skeletal and cardiac muscle (Brunori 2001; Frauenfelder et al. 2001). Myoglobin is largely accepted as a model system to investigate subtle details of protein dynamics and the connection to function. In the active centre of Mb the heme iron [in the Fe(II) or Fe(III) state] binds to four pyrrole nitrogens of the protoporphyrin IX and the imidazole nitrogen Nϵ of the proximal histidine F8 (Takano 1977a, 1977b; Perutz 1979; Phillips 1980). The sixth position at the iron at the distal side of the heme is unoccupied in deoxymyoglobin (Mbdeoxy) or occupied by a ligand. Small ligands such as $O_2$ and CO can bind to Fe(II); a water molecule ligates Fe(III) in metmyoglobin (Mbmet). An important functional role belongs to the distal histidine 64 (His64). It is supposed to control one possible way for the water to enter the distal heme cavity (Kachalova et al. 1999). The ligations of the iron by $O_2$ in oxymyoglobin and $H_2O$ in Mbmet are stabilized by a hydrogen bond to the histidine Nϵ (Olson and Phillips 1997; Phillips and Schoenborn 1981). Mutations of His64 to hydrophobic residues lead to a loss of the water ligand in Mbmet (Quillin et al. 1993).

Optical measurements on the heme chromophore are well suited to deduce the ligation and the spin state of the iron (Makinen and Churg 1983). As the heme contains an iron atom, myoglobin can be investigated by

Mössbauer spectroscopy. Protein dynamics have been determined from the temperature dependence of the Lamb-Mössbauer factor and the Debye-Waller factor (Parak and Formanek 1971; Chong et al. 2001). Deep insight into the dynamics and function of myoglobin has been obtained by flash photolysis of the CO in CO-ligated myoglobin solution (Austin et al. 1975). The terms "complexity" and "energy landscape" as general concepts for proteins are the result of numerous intensive investigations (Frauenfelder et al. 1988, 1999).

In myoglobin, Mössbauer spectroscopy revealed a dramatic change of the temperature dependence of the mean square displacement, $< x^2 >$, at the position of the iron at 180–200 K (Parak and Formanek 1971; Keller and Debrunner 1980; Parak et al. 1981). This effect, which is now called the "dynamical transition", has been observed also by many other experimental techniques like infrared spectroscopy (Ansari et al. 1987), neutron scattering (Doster et al. 1989), flash photolysis (Steinbach et al. 1991), time-resolved hole burning (Shibata et al. 1998), and the temperature dependence of the X-ray structure of photolysed MbCO (Ostermann et al. 2000). The dynamical transition has also been found by incoherent neutron scattering in other proteins like bacteriorhodopsin (Reat et al. 1998) and superoxide dismutase (Andreani et al. 1995) or by Mössbauer spectroscopy in photosynthetic reaction centres (Parak et al. 1980) or HiPIPs (Dilg et al. 2002). Below the transition the dynamics can be described in a good approach by normal modes (Melchers et al. 1996; Achterhold et al. 2002). At higher temperatures, protein-specific motions set in.

Important information on the dynamics of conformational changes can be obtained by the study of intermediate states generated at cryogenic temperatures. Earlier we have shown that the reduction of sperm whale (sw) Mbmet at low temperatures produces intermediate states of myoglobin where the reduced Fe(II) is low spin (Prusakov et al. 1995; Lamb et al. 1998; Engler et al. 2000). The metastable low-spin state has been characterized by X-ray structure analysis (Engler et al. 2000). The low-spin intermediate state Fe(II)Mb$H_2O$ is metastable below 140 K but relaxes at higher temperatures to the equilibrium high-spin Mbdeoxy after dissociation of the $H_2O$. The relaxation is non-exponential in time and is completed at about 200 K. Stability of the low-spin complex of heme Fe(II) with the water molecule in Fe(II)Mb$H_2O$ can be ascribed to a certain degree to the stabilization of the water by its hydrogen bond with His64.

In the following we describe studies of the mutant H64V of sw Mb where His64 is replaced by the nonpolar valine, which cannot form a hydrogen bond. In the H64V-Mbmet, no water is found at the iron(III) at room temperature. To obtain more information on the water bonding, optical absorption spectra in the Soret band from 300 to 20 K have been measured. To investigate the change of the ligation, the X-ray structures above and below the dynamical transition temperature were determined. A metastable low-spin intermediate Fe(II) state of the H64V was produced at low temperature by reduction of the H64V-Mbmet with thermalized electrons and was studied by Mössbauer spectroscopy.

## Materials and methods

### Preparation of the sw myoglobin mutant H64V and crystals

A Tb-1, pMb413 *Escherichia coli* strain was obtained from Prof. G.U. Nienhaus (Abteilung Biophysik, Universität Ulm, Germany). It contains an expression vector pUC19 with the synthetic gene for production of H64V myoglobin. The bacteria were grown and the protein was purified as described by Springer and Sligar (1987). The anion exchange chromatography was performed on a HiLoad 16/10 Q Sepharose column (Pharmacia, Germany, 1 M NaCl, 20 mM Tris, pH 8.4) and the gel permeation on a HiLoad 16/60 Superdex 75 prepgrade column (Phamacia, Germany, 50 mM $NaH_2PO_4$, pH 6.0). Finally, a cation exchange was performed (Hi Load 16/10 SP Sepharose, Phamacia, Germany, 50 mM $NaH_2PO_4$, pH 6.0). The Soret band of the purified protein showed the broad band characteristic for the five-ligated H64V-Mbmet state [cf. Morikis et al. (1990) and Fig. 1a]. No oxidation of the heme was necessary. For Mössbauer measurements the H64V-Mbmet was enriched with $^{57}$Fe and crystallized.

The samples of H64V-Mbmet for the optical measurements were prepared according to Lamb et al. (1998). The protein concentration was 5 mM H64V-Mb in 50 mM potassium phosphate buffer (Merck, Darmstadt, Germany) in a mixture of 50% (vol/vol) glycerol (Fluka, Buchs, Switzerland) at pH 7.0. A second sample was prepared from native sperm whale myoglobin (Sigma, St. Louis, Mo., USA) in the same way.

To crystallize the protein, a solvent was prepared containing 50 mM $KH_2PO_4$, 2.9 M $(NH_4)_2SO_4$ at pH 6.8. The protein concentration was set to 30 mg/mL. The samples were seeded with crushed crystals from native sperm whale myoglobin in the space group $P2_1$. After some weeks, crystals of acceptable size and shape were grown. They were isolated from the rest and the solution was purged with 50 mM $KH_2PO_4$, 2.9 M $(NH_4)_2SO_4$ at pH 6.8 to remove the protein from the solvent. Subsequently the solvent was exchanged slowly to 50 mM $KH_2PO_4$, 2.9 M $(NH_4)_2SO_4$ at pH 6.8 with 0.8 M trehalose (Roth, Karlsruhe, Germany) as cryoprotectant. To obtain Mössbauer samples the H64V-Mbmet crystals were dissolved in a mixture glycerol/0.1 M potassium phosphate buffer (1:1, vol/vol). The protein concentration was ~5 mM at pH 7.0.

### X-ray diffraction: data collection and refinement

The crystal for the X-ray diffraction at 300 K was kept in a capillary. For the measurement at 110 K, another crystal was prepared in a loop as described by Teng (1990) and Gamblin and Rodgers (1993). The crystal was caught in the loop with a drop of mother liquor and quickly transferred into the cryo-stream, which was set to a temperature of 110 K.

Reflection intensities were collected on an Enraf Nonius FR591 rotating anode using a Siemens Histar multiwire proportional counter mounted on a three-circle diffractometer. The intensities of the reflections were integrated and scaled by the program SAINT

**Fig. 1** **a** Optical absorption spectra of H64V-Mbmet in 50% glycerol/water as a function of temperature from 295 K down to 20 K (every 20 K). **b** Optical absorption spectra of H64V-Mbmet dried in trehalose as a function of temperature from 300 K to 20 K (every 20 K). **c** As example, the fitting of the 180 K spectrum from **a** according Eq. (1): *dashed line*: H64V-Mbmet at 295 K; *dotted line*: native Mbmet at 20 K; *solid line*: sum of the two subspecies; *circles*: absorption spectrum of H64V measured at 180 K

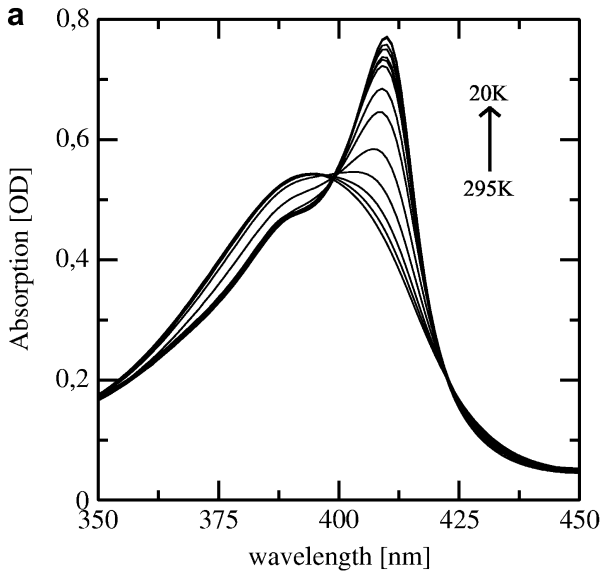


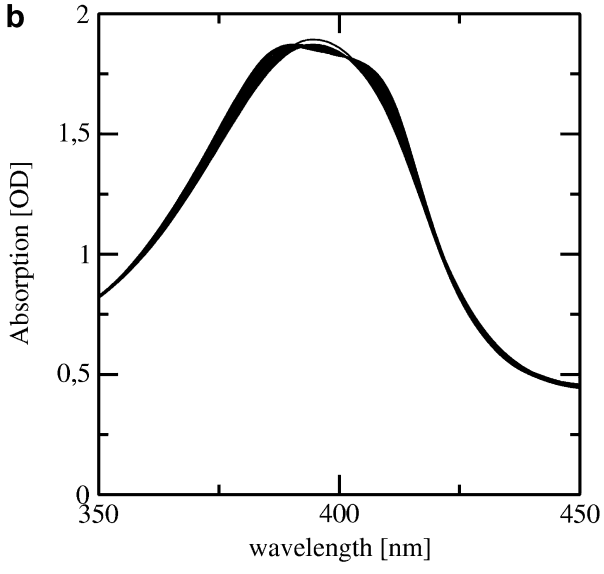


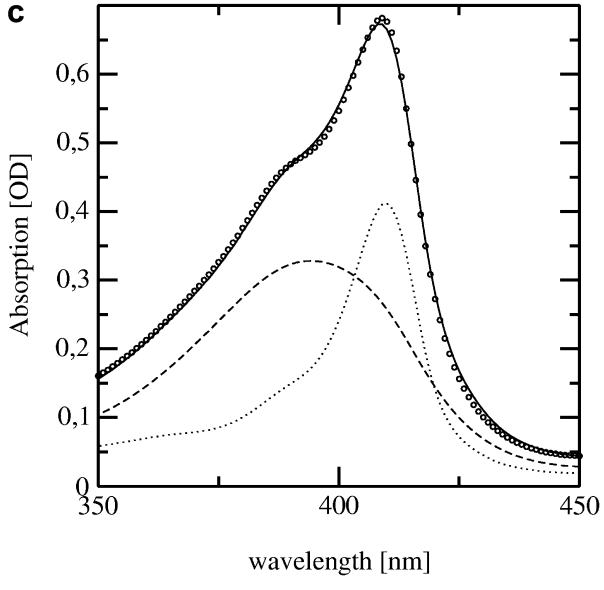


(Siemens). Subsequent data reduction was performed by the CCP4 programs AGROVATA and TRUNCATE (Bailey 1994). The refinement was done using the program X-PLOR 3.1 and 3.851 (Brünger 1992). The structure of Mbmet at 115 K (Engler et al. 2000) was used as the starting model. For both structure refinements the position of the water molecule which coordinates the heme iron was not restrained to the iron or any other part of the protein molecule, neither by bonded nor by nonbonded interaction. The water that can be found inside the heme pocket at low temperature next to the ligating water was also not restrained. No angle restraints were used for the proximal histidine with respect to the iron atom. The bond restraints for the proximal histidine bond as well as for the pyrrole nitrogen bonds to the iron were weakened from the standard X-PLOR values to allow an almost unrestrained refinement of this region. Water molecules and alternate conformations of side chains were included in subsequent refinement cycles after inspection of the electron density maps. The positions of the active-site atoms and the amino acids, which were modelled with alternate conformations, were verified by calculated, simulated annealing omit maps (Hodel et al. 1992).

### Optical absorption measurements

For the optical absorption measurements a drop of 2 μL of protein solution was loaded between two fused silica windows (1 mm thick) separated by a 12 μm spacer. The copper sample cell was loaded in a Leybold closed-cycle helium refrigerator (RDK 10-320, Hanau, Germany) equipped with a top-loading cell. The sample chamber was filled with helium to act as a thermal contact gas. The temperature was measured to $\pm 1$ K using a silicon temperature diode (DT-471, Lakeshore Cryogenics, Westerville, Ohio, USA) mounted on the sample cell near to the sample and a Leybold LTC 60 temperature controller. A Perkin-Elmer Lambda 19 spectrometer (Überlingen, Germany) was modified to allow contact-free mounting of the cryostat within the spectrometer. The spectra were collected with a slit width of 1 nm, 120 nm/min scan speed and 2 nm smoothing.

### Mössbauer studies

The samples with a thickness of 4 mm were tightly closed in PVC holders by indium-sealed Mylar windows. X-ray irradiation of the samples was performed at 85 K, employing a copper X-ray tube without a monochromator running at 40 kV and 30 mA. The total irradiation lasted for 90 h. To provide a uniform X-ray irradiation the sample was rotated by 180° after half of the irradiation time. As in the case of native myoglobin (Prusakov et al. 1995), the temperature dependence of the relaxation of the H64V intermediate states produced by the irradiation was studied using the temperature cycling procedure: the sample was heated in the Mössbauer cryostat to a temperature $T_i > 80$ K with a rate of 2–3 K/min and kept at $T_i$ for 45 min. Then the sample was cooled at a rate of 2–5 K/min and its Mössbauer spectrum was measured at 80 K. The cycle was repeated with $T_{i+1} > T_i$. A $^{57}$CoRh source and a conventional electromagnetic drive system with a sinusoidal velocity profile were used to measure the Mössbauer spectra. The temperature of the samples was adjusted with an error better than $\pm 2$ K. The Lamb-Mössbauer factor of the different iron species were assumed to be equal at 80 K. The values of the isomer shifts are given relative to metal iron (α-Fe) at room temperature.

## Results

### Optical absorption spectroscopy

The results of the optical absorption spectroscopy as a function of temperature are shown in Fig. 1a for the

H64V in solution and in Fig. 1b for H64V-Mbmet dried in trehalose. A linear baseline was subtracted from all spectra. At 295 K the absorption spectra show only one broad band with its maximum at 394 nm. While in the trehalose-coated sample the spectra did not depend on temperature, the first sample showed an increasing peak at 410 nm upon lowering the temperature. There is a clear isosbestic point at 399 nm, which indicates the temperature-dependent equilibrium between two species. Below 180 K the spectra change only slightly. Assuming that the spectrum at 295 K is caused by 100% of the five-ligated heme and that the spectrum of the species showing the Soret band at 410 nm is the same as for native six-ligated metmyoglobin, the spectra were fitted with a superposition of these spectra as a function of temperature:

$$A(\lambda, T) = c_{394}(T)A_{394}(\lambda, T = 295\ \mathrm{K}) + c_{410}(T)A_{410}(\lambda, T = 20\ \mathrm{K}) \quad (1)$$

where $c$ denotes the relative concentration and $A$ the absorption of the species, respectively. The absorption maximum is indicated by the subscript. Neglecting a possible temperature dependence of the spectral shape of the two components, one obtains fits as shown in Fig. 1c. As we do not have an extinction coefficient for the species with the absorption maximum at 410 nm, we have to introduce a scaling factor $c_{sc}$ for this species to obtain the relative amount of both species:

$$c_{410}(T) = c^*_{410}(T)c_{sc} \quad (2)$$

The scaling factor is assumed to be temperature independent and the total amount of protein should be constant for all temperatures. Thus we can minimize the difference of the total protein concentration $c_{tot}$ from a constant value, in order to determine the scaling factor, where:

$$c_{tot}(T) = c_{394}(T) + c^*_{410}(T) \quad (3)$$

In this way we obtained a mean relative protein concentration of 1.013 (instead of 1.000) averaged over all spectra from 20 K to 295 K. The standard deviation was 0.010. The percentage of the species with the peak at 394 nm as a function of temperature is shown in Fig. 2a. The equilibrium between the two species:

$$\mathrm{H64V-Mbmet} \overset{K}{\rightleftharpoons} \mathrm{H64V-MbmetH_2O} \quad (4)$$

determines the equilibrium constant $K$:

$$K = \frac{c_{394}}{c_{410}} \quad (5)$$

where $K$ is related to the enthalpy $\Delta H$ and entropy $\Delta S$ differences:

$$K = \mathrm{e}^{-\Delta G/(RT)} = \mathrm{e}^{-(\Delta H - \Delta ST)/(RT)} \quad (6)$$

The amount of the species with the Soret band at 394 nm does not decrease to zero upon lowering the temperature, showing that the equilibrium could not be reached. Thus we can only model the data with Eq. (5) in a certain temperature range. A satisfying fit is obtained in the high-temperature region. Below about 220 K the deviation from equilibrium becomes significant (compare Fig. 2a and b). The fit to Eq. (5) yields $\Delta H = 22$ kJ/mol and $\Delta S = 106$ J/(mol K).

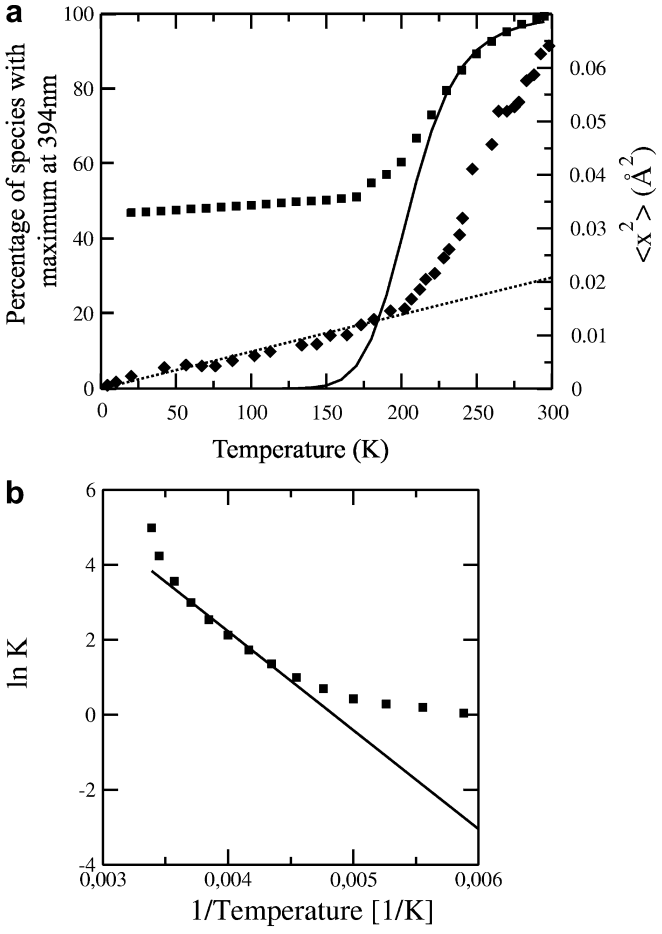


**Fig. 2** **a** Percentage of the species with the Soret band maximum at 394 nm, the five ligated species, as a function of temperature. *Solid squares*: data evaluated according to Eq. (1) (cf. Fig. 1c). *Solid line*: fit according to Eq. (5). *Solid diamonds*: mean square displacement of iron atoms in Mbdeoxy obtained from Mössbauer spectroscopy (Parak et al. 1982). *Dotted line*: linear temperature dependence of the harmonic vibrations. **b** ln$K$ versus $1/T$: symbols are the same as in **a**

## X-ray structure analysis

To reveal the structural details of the observed spectral changes, an X-ray structure analysis at 300 K and 110 K was performed. The 110 K data set has been measured up to 1.3 Å and the 300 K data set up to 1.5 Å The crystals had a size of 0.4×0.7×0.7 mm$^3$ at 110 K and 0.4×1.0×1.0 mm$^3$ at 300 K. Each data set was measured with one crystal. No radiation damage was observed either at low or at high temperatures. Information on

data for the data collection and refinement is given in Table 1.

Figure 3 shows the obtained structures in the region of the active centre. A weighted $2mF_o$–$DF_c$ map contoured at $1.5\sigma$ (Bailey 1994) is shown. At 300 K the heme is five ligated. No water molecules can be found in the heme pocket (Fig. 3a). Lowering the temperature leads to a well-defined water structure in the heme pocket, stabilizing a water at the sixth coordination position (Fig. 3b). The three closest waters to the heme iron are modelled with the same occupancy and different *B*-factors. As there is a correlation of *B*-factor and occupancy (Carugo 1999), the occupancy was fixed to 0.5 as determined by the optical spectra for the iron-bound water. The refined *B*-factor for the water nearest to the iron atom is close to the *B*-factor observed for the iron. For the determination of a possible occupancy of the water ligating the heme iron even at room temperature, we fixed the *B*-factor to the one observed for the heme iron and determined an occupancy of 36%. We also put waters on the protein surface, where no electron density at $1\sigma$ could be observed. Subsequently, we refined their occupancy for a *B*-factor of the value obtained for the heme iron. The results varied between 0% and 7%. Thus the value of 36% is a significant occupancy.

For the heme plain, a weighted $2mF_o$–$DF_c$ map was calculated contoured at $1.5\sigma$ as well as a weighted $mF_o$–$DF_c$ map (contoured at $3\sigma$ and $-3\sigma$). The low-temperature $mF_o$–$DF_c$ map gave strong evidence for two positions of the heme linked by a sliding motion within the heme plane. A similar feature was not observed in the room temperature data.

To reveal changes of the overall structure upon changing the temperature, we have calculated a matrix of the distances of the main-chain centroids for each structure calculated. The subtraction of these distance matrices for different structures yields so-called delta distance plots. The delta distance plots for the mutant protein calculated for the structures at 300 K and 110 K look very similar to the one obtained for the native protein. Calculating a matrix of the absolute value of the delta distance matrix of the native protein minus the delta distance matrix for the mutant shows an overall bigger expansion of the mutant compared to the native protein. In other words, upon cooling, the mutant contracts stronger than the native protein. This is in accordance with the bigger contraction of the mutant as measured by the unit cell parameters. The delta difference plots between the native and the mutant protein at the respective temperatures are also very similar, showing the strongest difference in the CD loop at lysine 47. At low temperature the differences are bigger but uniformly spread over the whole protein, which can be attributed to the larger contraction of the mutant protein. We also could not find

**Table 1** Data collection and refinement statistics. Values in parentheses refer to the highest resolution shell, 1.55–1.5 Å for H64V-Mbmet at 300 K and 1.35–1.3 Å for H64V-Mbmet at 110 K. $R_{merge} = \Sigma_{hkl}\Sigma_j|I_j - < I >|/\Sigma_{hkl}\Sigma_j < I >$, where $I_j$ is the intensity $I$ for the $j$th measurement of the reflection with indices $hkl$ and $< I >$ is the mean of all measurements of the reflection $I$. $R_{cryst} = \Sigma_{hkl}|F^o_{hkl} - F^c_{hkl}|/\Sigma_{hkl}|F^o_{hkl}|$, where $F^c_{hkl}$ and $F^o_{hkl}$ are the observed and calculated structure factor amplitudes for the reflection $hkl$. $R_{free}$ is the crystallographic $R$ value calculated with the structure factor amplitudes of the test set which is not involved in the refinement calculations. The given overall coordinate error was estimated by a $\sigma_A$ plot (Read 1986). For the calculation of the distance Fe-< heme plane > and Fe-$< N_{plane} >$ the planes are defined as the best-fit planes through the 20 central C-atoms of the heme and the four heme N-atoms, respectively

| | 110 K | | 300 K | |
|---|---|---|---|---|
| Data collection | | | | |
| Space group | $P2_1$ | | $P2_1$ | |
| Unit cell (Å or °) | $a = 63.91$, $b = 30.63$, $c = 34.32$, $\beta = 105.6$ | | $a = 64.89$, $b = 30.87$, $c = 34.86$, $\beta = 105.8$ | |
| Resolution (Å) | 10.0 to 1.3 | | 10.0 to 1.5 | |
| Measured reflections | 107,379 | | 68,990 | |
| $< I > / < \sigma(I) >$ | 11.7 | | 12.4 | |
| Unique reflections | 29,970 | | 20,771 | |
| Completeness overall (%) | 94.5% (83.4%) | | 96.6% (92.0%) | |
| $R_{merge}$ (%) | 3.5% | | 3.6% | |
| Refinement | | | | |
| Resolution range | 7.0 to 1.3 | | 7.0 to 1.5 | |
| Number of reflections | 29,963 | | 20,766 | |
| Working set/test set | 26,965/2998 | | 18,724/2042 | |
| $R_{cryst}$ (%) | 18.5 | | 17.5 | |
| $R_{free}$ (%) | 21.7 | | 21.0 | |
| R.m.s.d. of bond length (Å) | 0.009 | | 0.006 | |
| R.m.s.d. of bond angles (°) | 1.104 | | 1.018 | |
| R.m.s. coordinate error (Å) | 0.13 | | 0.13 | |
| Geometry | H64V Mbmet | Native Mbmet | H64V Mbmet | Native Mbmet |
| Temperature (K) | 110 | 105 | 300 | 300 |
| Fe-$H_2O$ (Å) | 2.38 | 2.15 | – | 2.17 |
| Fe-His93 (Å) | 2.11 | 2.11 | 2.11 | 2.17 |
| Fe-< heme plane > (Å) | 0.25 | 0.14 | 0.33 | 0.12 |
| Fe-$< N_{plane} >$ (Å) | 0.18 | 0.08 | 0.23 | 0.06 |

significant differences in the *B*-factors as a function of temperature for the mutant as compared to the native protein.

One trehalose molecule of the buffer was visible in both structures with a *B*-factor of about 50. The trehalose molecule binds to the AB loop at the nitrogen backbones of residues 21 and 22. This position differs from the one observed for the space group *P*6 (Ostermann et al. 2000).

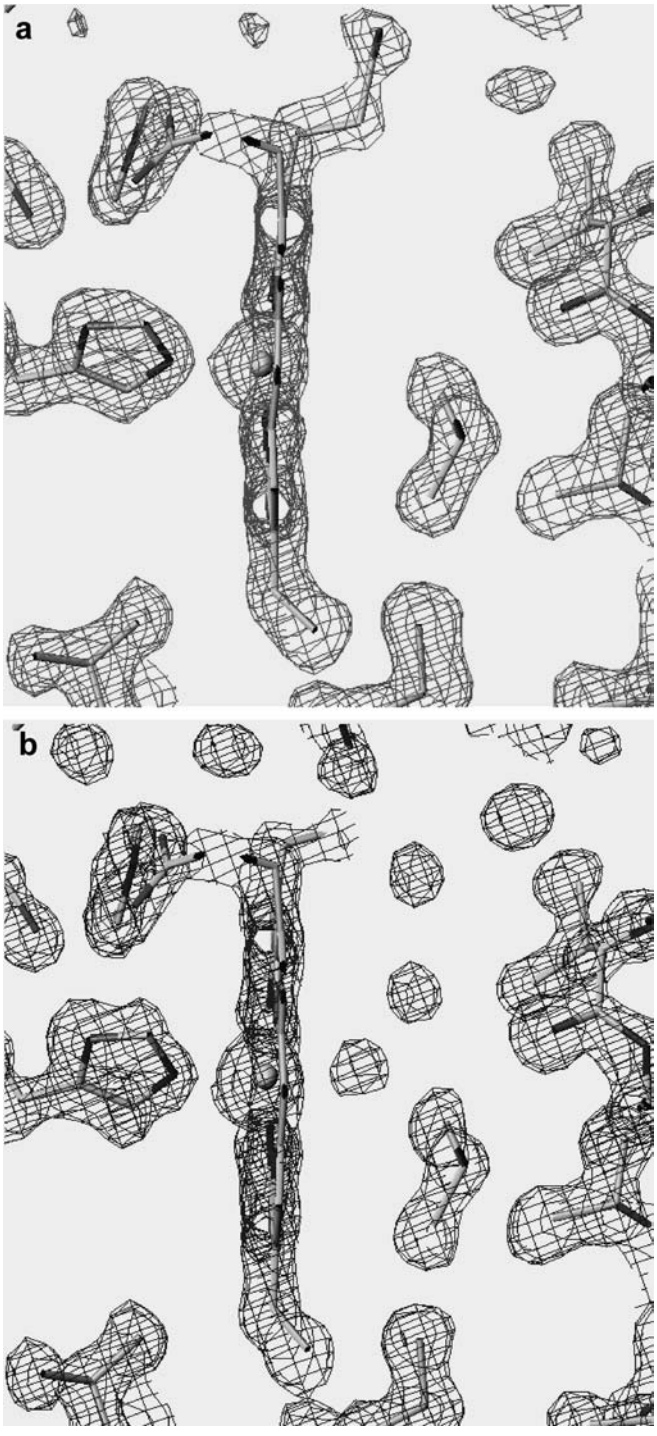


**Fig. 3** Side view of the heme pocket. Model and $2mF_o$–$DF_c$ map contoured at $1.5\sigma$: **a** 300 K; **b** 110 K. Note the water molecules in the heme pocket, visible at 110 K

## Mössbauer spectroscopy

### *Mössbauer spectroscopy of H64V-Mbmet*

Figure 4 gives the Mössbauer spectra of H64V-Mbmet before irradiation, measured at 5 K and 80 K with and without an external transversal magnetic field of 20 mT. The spectra are typical for a Fe(III) high-spin heme and similar to the corresponding spectra of the native Mbmet (Thomanek et al. 1977; Bizzarri et al. 1995). It was not possible to resolve the two states of H64V-Mbmet (with five- and six-coordinate iron) as observed in the low-temperature optical spectra.

### *Low-temperature reduction of H64V-Mbmet*

X-ray irradiation of the H64V-Mbmet sample at 85 K results in a drastic change (Fig. 5). The spectra of the irradiated H64V-Mbmet at 80 K with and without an external magnetic field are identical, indicating a complete reduction of the high-spin iron(III).

The spectrum of the irradiated H64V-Mbmet can be well fitted by a superposition of four symmetrical doublets. Their parameters are given in Table 2. The fraction of doublet 1 with the Mössbauer parameters of the low-spin Fe(II) is only about 30%. The main

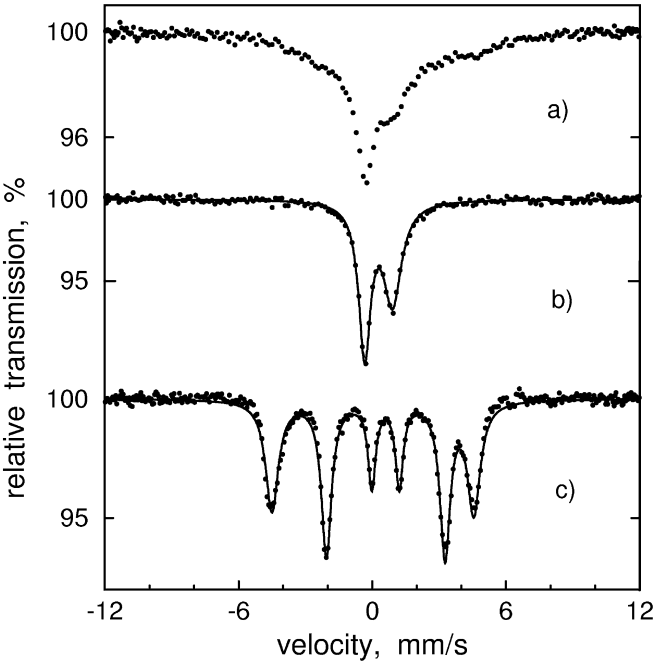


**Fig. 4** Mössbauer spectra of H64V-Mbmet before X-ray irradiation: (*a*) without a magnetic field at $T = 80$ K; (*b*) and (*c*) in a transverse magnetic field of 20 mT at 80 K and 5 K, respectively

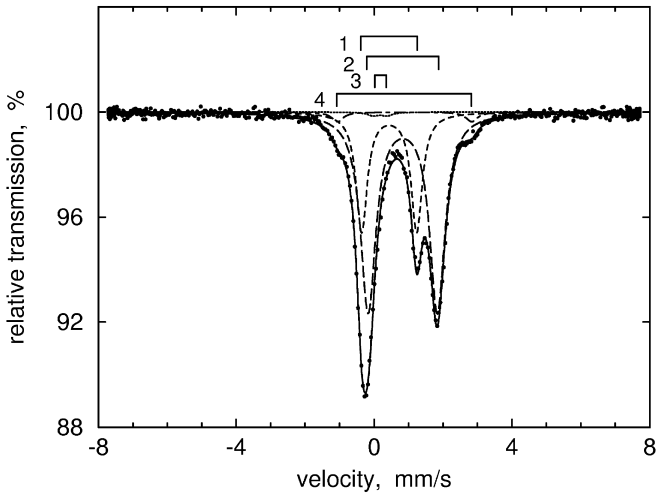


**Fig. 5** Mössbauer spectrum at $T = 80$ K in transverse magnetic field of 20 mT for H64V-Mbmet after irradiation. Interpretation with four iron species

component (~66%) of the spectrum is doublet 2 of high-spin Fe(II), with the parameters close to those for H64V-Mbdeoxy obtained by chemical reduction. The less intense doublet 3 has parameters typical for MbCO. Doublet 4 has the isomer shift of high-spin Fe(II) but a much larger quadrupole splitting than H64V-Mbdeoxy.

*Relaxation of the intermediate state*

As in the case of the native myoglobin, the relative fractions of the iron species produced by irradiation do not vary for more than a month if the samples are kept in liquid nitrogen. Figure 6 shows Mössbauer spectra of the irradiated H64V-Mbmet after warming up to excursion temperatures, $T_i$, using the described temperature cycling procedure. The corresponding change of the relative fractions of the iron species with rising $T_i$ is presented in Fig. 7. Upon warming to 100 K, nothing happens. At 115 K the fraction of low-spin Fe(II) begins to decrease, whereas that of the Fe(II) high-spin A species increases. Up to about 170 K this tendency continues: the low-spin Fe(II) species decreases and disappears at about 170 K. Essentially, this is compensated by the increase of the Fe(II) high-spin A species. The fraction of Fe(II) high-spin B species does not change up to 160 K. Above 160 K the fractions of both the Fe(II) high-spin forms decrease dramatically and the small contribution of Fe(II) high-spin B disappears totally. The MbCO component increases sharply. Above 180 K the sample contains the same amount of MbCO and Fe(II) high-spin A. Note that the fraction of MbCO species slightly increases from 80 K to 160 K.

Figure 8 shows the relative fractions, $N_T$, of the intermediate Fe(II) low-spin states of the native and mutant myoglobins as a function of the excursion temperature $T_i$. $N_T$ is normalized to one for the fraction obtained immediately after irradiation. As for the native myoglobin (Parak and Prusakov 1994), the experimental data for the mutant protein cannot be described with a single activation barrier height. Earlier we used a simplified approach with the barrier height distribution $g(H^*)$ described by Zollfrank and Friedrich (1990). The approach assumes that for each $T_i$ a threshold barrier $H_T^*$ exists that can be overcome within $\tau_{exp}$ (45 min in our cases). All protein molecules in conformational substates with $H^* < H_T^*$ relax, whereas those with $H^* > H_T^*$ remain in the metastable intermediate state. In this approach the fraction of the protein molecules remaining in the intermediate Fe(II) low-spin state after keeping the sample during $\tau_{exp}$ at $T_i$ is given by:

$$N_T \approx \int_{H_T^*}^{\infty} g(H^*)\,\mathrm{d}H^* \tag{7}$$

The protein substates with $k^{-1} < \tau_{exp}$ can relax and the barrier $H_T^*$ is determined by the condition:

$$k^{-1} \approx \tau_{exp} \tag{8}$$

With the Arrhenius relation for the relaxation rate, $k = k_0 \exp(-H^*/RT)$, one obtains:

$$H_T^* = RT \ln(k_0 \tau_{exp}) \tag{9}$$

**Table 2** Isomer shift, IS, quadrupole splitting, QS, and relative fraction, $P$, of the different iron species produced at low-temperature X-ray irradiation of sw Mbmet and H64V-Mbmet. $T_{meas} = 80$ K. The sw Mbmet data are taken from Prusakov et al. (1995). The last two lines represent chemically reduced samples

| Species | Mbmet | | | H64V-Mbmet | | | Iron state |
|---|---|---|---|---|---|---|---|
| | $IS_{\alpha\text{-Fe}}$ (mm/s) (±0.02) | QS (mm/s) (±0.03) | $P$ (%) (±1) | $IS_{\alpha\text{-Fe}}$ (mm/s) (±0.02) | QS (mm/s) (±0.03) | $P$ (%) (±1) | |
| 1 | 0.55 | 1.53 | 89 | 0.55 | 1.58 | 29 | Fe(II) low spin |
| 2 | 1.08 | 2.04 | 8 | 0.94 | 2.00 | 66 | Fe(II) high spin A |
| 3 | 0.29 | 0.32 | 3 | 0.29 | 0.40 | 2 | MbCO/H64V-MbCO |
| 4 | | | | 1.01 | 3.90 | 3 | Fe(II) high spin B |
| Mbdeoxy | 0.89 | 2.19 | | | | | Fe(II) high spin |
| H64V-Mbdeoxy | | | | 0.90 | 2.01 | | Fe(II) high spin |

A reasonable fit of the relaxation data for both the native and the mutant myoglobin is achieved with a Gaussian distribution of the barrier height:

$$g(H^*) = \left(2\pi\sigma^2\right)^{-1/2} \exp\left[\frac{-\left(H^* - H_0^*\right)^2}{2\sigma^2}\right] \qquad (10)$$

where $\sigma$ is the width of the corresponding distribution and $H_0$* is the position of its centre.

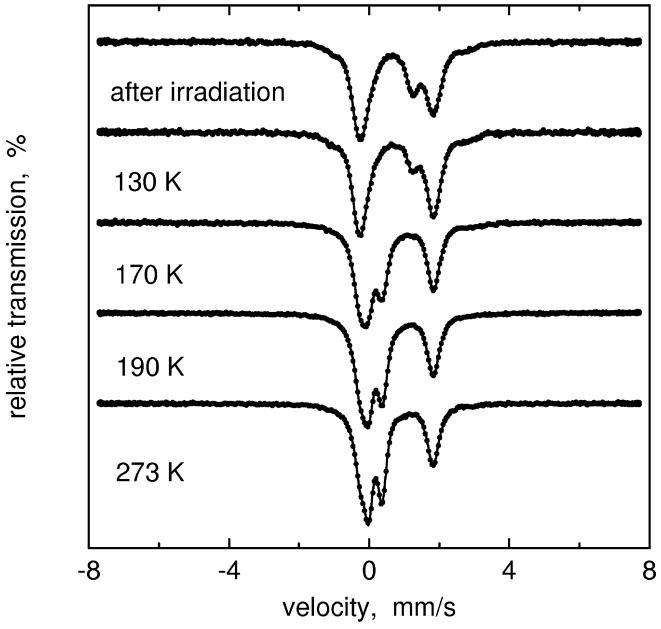


**Fig. 6** Mössbauer spectra at $T = 80$ K of the irradiated H64V-Mbmet after different excursion temperatures, $T_i$. The sample was kept 45 min at $T_i$

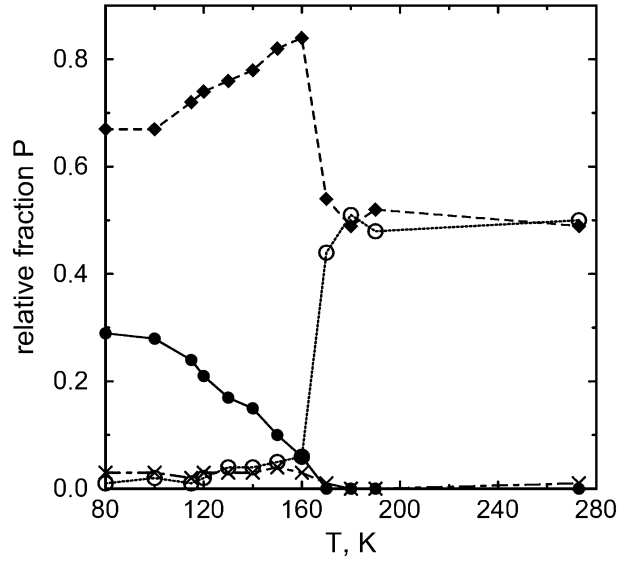


**Fig. 7** Relative fraction, $P$, of the observed iron species in the irradiated H64V-Mbmet as a function of the excursion temperature, $T$. *Solid circles*: Fe(II) low-spin; *diamonds*: Fe(II) high-spin A species; *crosses*: Fe(II) high-spin B species; *open circles*: H64V-MbCO

The thermal cycling experiments without kinetic studies do not allow us to determine $k_0$. To evaluate the data independent of $k_0$ one may insert Eq. (9) into Eq. (10). With this expression we can evaluate Eq. (7), where the width of the Gaussian $\xi = \sigma/(R\ln(k_0\tau_{exp}))$ and the barrier height are given in units of $T$:

$$N_T = \frac{1}{\sqrt{2\pi}\xi} \int_{T^*}^{T=\infty} \exp\left[-\frac{(T - T_0)^2}{2\xi^2}\right] dT \qquad (11)$$

Figure 8 and Table 3 represent the fit of the experimental data for the native and mutant myoglobins using Eq. (11). One can see that the distribution of the activation barriers for the mutant myoglobin has an essentially larger width and is 30 K shifted to lower temperatures in comparison with the native Mb.

Concomitant with the relaxation of the intermediate low-spin Fe(II) to the high-spin state, the quadrupole splitting and isomeric shift of the latter change (QS: from ~1.95 to ~2.15 mm/s; IS: from ~1.08 to ~0.89 mm/s). The evolution of the quadrupole splitting and isomeric shift of high-spin Fe(II) with increasing $T_i$ is shown in Fig. 9.

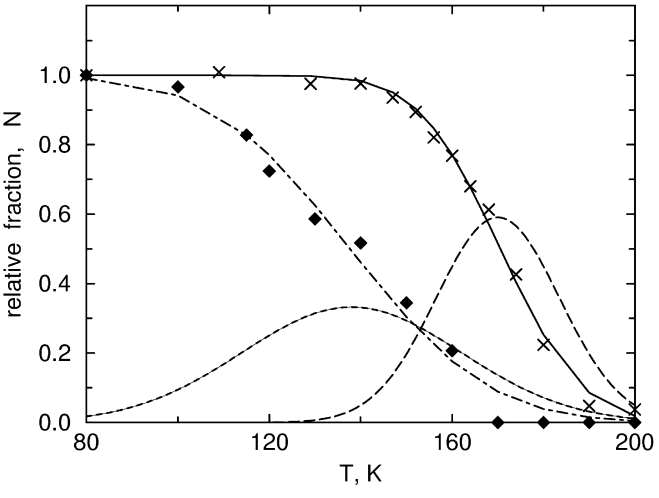


**Fig. 8** Fraction of the intermediate Fe(II) low-spin species in sw Mb (*crosses*) and H64V-Mb (*diamonds*) as a function of the excursion temperature. *Solid* and *dashed-dotted lines*: least squares fit for sw Mb and H64V-Mb, respectively, using Eq. (11) with Gaussian barrier height distributions shown as *dashed lines*

**Table 3** Parameters of the Gaussian distribution of the activated barriers (centre, $T_0$*, $H_0$* and width, $\xi$, $\sigma$) used to fit the relaxation of the intermediate 1s Fe(II) state of the native and H64V myoglobin (Eq. 11). The distributions are shown in Fig. 8

| | $T_0$* (K) | $\xi$ (K) | $H_0$* (kJ/mol) | $\sigma$ (kJ/mol) |
|---|---|---|---|---|
| sw Mbmet | 170 | 13.5 | 52 | 4.9 |
| H64V-Mbmet | 138 | 24 | 42 | 8.7 |

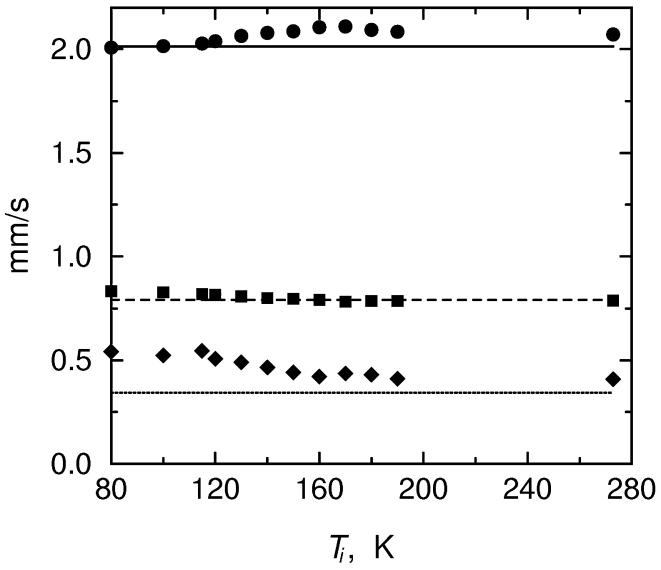


**Fig. 9** Isomer shift, IS (*squares*), quadrupole splitting, QS (*circles*), and linewidth, $\Gamma_{1/2}$ (*diamonds*), for the Fe(II) high-spin A component as a function of the excursion temperature, $T_i$; $T_{meas} = 80$ K. IS (*dashed line*), QS (*straight line*), and $\Gamma_{1/2}$ (*dotted line*) for H64V-Mbdeoxy at $T = 80$ K

## Discussion

### Influence of the crystal form on the stability

The structures of mutant myoglobin presented here were obtained at high resolutions. Structures of myoglobin mutants found in literature were exclusively determined with crystals in the space group *P*6 at lower resolution. The crystals of the space group $P2_1$ contain considerably less solvent, 37% compared to 62% in *P*6, concomitant with a higher packing density of the protein molecules. This might also be an explanation for the higher stability of $P2_1$ crystals against radiation damage. Quillin et al. (1993) reported the need for up to five crystals to measure one full data set, in contrast to our experiments. We found that the $P2_1$ crystals with trehalose included in the mother liquor are stable over months, whereas *P*6 crystals degenerate in the presence of trehalose within a few days.

### The transition from five-ligated to six-ligated heme in H64V-Mbmet

Let us first look at the optical absorption data. The spectra clearly indicate a transition as a function of temperature. As we can model all spectra by a superposition of a room-temperature spectrum of H64V, which is known to be indicative of a five-ligated heme, and a native Mbmet-spectrum, indicative of a six-ligated heme, the origin of the transition can be assigned to a change in ligation state. This is in agreement with the findings on other different met-myoglobin mutants, where also a mixture of the ligation state has been assumed (Tada et al. 1998). At this point we want to emphasize the little amount of change upon cooling below 180 K. The spectra do not change any more in the contribution of the two species but only show a temperature-dependent narrowing of the Soret band by freezing out vibrations which contribute to the bandwidth. From the X-ray structure analysis we can explain the mechanism of the transition. At room temperature the heme is mainly five ligated. The mechanism which leads to a stabilization of the water coordinating the heme iron is shown by the crystal structure at 110 K. The well-resolved peaks in the electron density displayed in Fig. 3b show the hydrogen bonding network of the water molecules stretching from the charged amino acids on the protein surface into the heme pocket. As the temperature is lowered the thermal energy and mobility of the water molecules is reduced and they even can become trapped in the shallow potential wells exerted by the surrounding protein residues and the hydrogen bonds with their neighbouring water molecules. The two water molecules closest to the water molecule ligating the heme iron are located close to the position of the histidine in the native protein. The distance between the ligating water to the first stabilizing water is only 2.6 Å. This water is 2.6 Å away from the next one. Nevertheless, the distance of the ligating water from the iron in native Mbmet is 2.2 Å, whereas it is 2.4 Å in the mutant.

A similar situation has been observed in the H64G mutant, where the distal histidine is exchanged to glycine (Quillin et al. 1993). Here the ligating water molecule is also stabilized by a second water molecule. The oxygen atom of this water molecule is located only 2.9 Å from the backbone oxygen atom of residue 64 and is thus stabilized by a hydrogen bond. The corresponding distance in our low-temperature structure for H64V is 3.3 Å, which is indicative of only weak hydrogen bonding. This second water in H64V is stabilized by a third water on the way from the heme pocket to the protein surface, which is not observed in H64G by Quillin et al. (1993). This third water is only 2.6 Å away from the second water and takes part in a hydrogen bonding network stretching along the surface of the protein. Thus the mechanism of stabilization of the ligating water molecule is maintained by a water network reaching into the heme pocket.

Besides the change in the water structure at the protein surface and within the heme pocket, no significant structural changes can be observed. The transition from five- to six-ligated is not significantly correlated with structural changes of the protein. Only a small heme shift is seen upon ligation. It is interesting to note that a heme shift was one of the main structural differences between the ligated states $MbO_2$, MbCO and Mbme-$tH_2O$ compared to Mbdeoxy in a recent X-ray structure analysis at very high resolution (Vojtechovsky et al. 1999). A heme shift is probably also involved in the

diffusion of the CO ligand after flash photolysis between the xenon holes (Tilton et al. 1984), as proposed by Chu et al. (2000). The de-ligation of the heme could thus lead to a shift of the heme which facilitates the diffusion of the ligand towards the proximal side, as also found by Ostermann et al. (2000).

The transition from the unligated to the water-ligated molecules is interrupted below 175 K, which is close to the dynamical transition temperature, $T_c$, found by Mössbauer spectroscopy in native myoglobin (Parak et al. 1982). Below this temperature the equilibrium described by Eqs. (4)–(6) is not reached any more (compare Fig. 2a). Thus the equilibrium between the ligation states correlates with the fluctuations between conformational substates as measured by Mössbauer spectroscopy. Mössbauer spectroscopy demonstrates that one has to deal with two different regions of protein dynamics. At low temperatures ($T < T_c$) a protein molecule is frozen into a conformational substate. The protein molecule vibrates essentially harmonically within its substate. Approaching the dynamical transition around 180 K, transitions between the substates become possible. Obviously, fluctuations between conformational substates are necessary to make possible a change between the two ligation states.

Measurements of the dielectric relaxation rate of adsorbed water in metmyoglobin crystals by Singh et al. (1981) show that these are correlated with the transition rates between conformational substates as determined by Mössbauer spectroscopy. This can be explained in the following way: fluctuations of the dipoles of water molecules can lower the barriers between conformational substates substantially by interactions with the polar amino acids on the protein surface. In a slightly different language, one may say that the fluctuating water molecules provide some of the enthalpy in order to reach the transition state between different conformational substates.

At this point we have to discuss the Mössbauer spectra shown in Fig. 4. As we have seen from optical spectroscopy and X-ray structure analysis, at low temperatures about 50% of the molecules are five-fold coordinated and the other 50% are six-fold coordinated. However, Fig. 4c shows only one species which is high-spin Fe(III) (Thomanek et al. 1977). In many heme compounds, six-fold coordinated iron is in the low-spin state. However, in the case of Fe(III), water is a weak ligand which is unable to force the iron into low spin. Since five-fold coordinated Fe tends to be high spin anyway, the dissociation of the water molecule does not change the spin state. Moreover, the quadrupole splitting as well as the isomer shift are very insensitive to this dissociation. For that reason the Mössbauer spectra in Fig. 4 cannot resolve the two ligation states. They reveal themselves only by line broadening. It is interesting to note that in the case of Fe(II) the different ligation states are well resolved by Mössbauer spectroscopy (compare Fig. 5).

### An intermediate state of H64V-Mbmet obtained by reduction, and its relaxation

After reduction by X-ray irradiation, 66% of the molecules go rapidly from the Fe(III) high-spin state into the Fe(II) high-spin equilibrium state, even at 80 K. This is reasonable for the five-fold coordinated Fe(III) molecules which represent 50% of the molecules in the sample. There is no water ligand which can stabilize the intermediate low-spin state. Sixteen percent of the water-ligated molecules relax also rapidly into the equilibrium state at 80 K, compared to only 8% in the native myoglobin. This can be explained by the weaker stabilization of the position of the heme-bound water by its hydrogen bond with the neighbouring water molecules. It is also reflected in the Gaussian barrier height distribution used to explain the relaxation process. As shown in Fig. 8, the distribution is not zero at 80 K. Molecules exist which can surmount the barrier easily below 80 K. Only 29% of the molecules become trapped in the intermediate state.

Three percent of the molecules are converted by irradiation into another intermediate state (species 4 in Table 2), with very large quadrupole splitting (QS = 3.9 mm/s). The Mössbauer parameters are characteristic of a five-coordinate Fe(II) high-spin porphyrin complexes where the iron atom is more than 0.5 Å displaced from the porphyrin plane to an axial ligand (Schappacher et al. 1983; Silver et al. 1984; Bill et al. 1988; Mandon et al. 1990; Bominaar et al. 1992). It is unclear if this state comes from an initial Fe(III) state having already a large out-of-plane shift of the iron, since different iron species could not be resolved from the Mössbauer spectra before irradiation.

A small fraction of molecules is ligated with CO immediately after the irradiation. These CO molecules may be produced within the heme cavity by radiation damage within the protein. However, since large time scales are involved in the investigation, the CO molecules may also have moved into the cavity from outside. As shown by X-ray investigations, CO may migrate within the protein moiety even at very low temperatures (Ostermann et al. 2000).

In H64V the dissociation of the ligating water from the low-spin Fe(II) starts already above 100 K (for sw Mb above 140 K) and is completed at about 170 K. This is significantly lower than the temperature of the dynamical transition of native myoglobin ($T_c \approx 180$ K). Does this mean that the correlation between water dissociation and protein specific dynamics is not valid in this case? There are two possible explanations. First of all, the dynamical transition temperature of the H64V mutant may be lower, as in native myoglobin. This has to be investigated in future. A more probable explanation comes from X-ray structure analysis. As shown in this paper, the structure of six-coordinated and five-coordinated Fe(III) high-spin H64V is equal. In native myoglobin the structure of the six-ligated Fe(III) high-spin state and the six-ligated Fe(II) low-spin state are

also equal (Engler et al. 2000). It seems reasonable that the structures of the five-coordinated intermediate H64V state and the five-coordinated deoxy state are also equal. The relaxation is then reduced to a movement of the water molecule. A structural relaxation of the protein moiety is unnecessary. It is well known from other experiments that small molecules can move within the protein matrix below $T_c$, e.g. compare Ostermann et al. (2000). Unfortunately, the structure of H64V-Mbdeoxy is not available as the autoxidation rate is very high (Quillin et al. 1993).

### Relaxation within the deoxy state

The final Mbdeoxy equilibrium state is not reached in one step. The change of the Mössbauer parameters of the Fe(II) high-spin species produced at low-temperature reduction of sw Mbmet and H64V-Mbmet (present data and Prusakov et al. 1995) demonstrates a slow local structural reorganization at temperatures above 120 K until the final equilibrium is reached. The changes of the quadrupole splitting and the isomer shift of the Fe(II) high-spin molecules with increasing $T_i$ (Fig. 9) have the same tendency but are smaller in H64V than in the native protein. A structural interpretation could be that the iron displacement out of the heme in H64V-Mbmet with water is already closer to the deoxy state than in native Mbmet. Earlier we have found (Lamb et al. 1998; Prusakov et al. 1999) that the Soret band of low-spin Fe(II) in the intermediate state of sw Mb is blue-shifted above ~100 K, demonstrating also slow structural rearrangements (Engler et al. 2000). These two facts together demonstrate that the so-called intermediate state as well as the equilibrium state is an average over many substates which are populated as a function of temperature and time.

### The dependence of $T_c$ on the time resolution of the experiment

In the literature the question is discussed if the dynamical transition is a physical property of the protein together with its environment or if it is more or less an artifact produced by the time resolution of each experiment (Daniel et al. 2003). While incoherent neutron scattering (Doster et al. 1989) and Mössbauer spectroscopy (Parak and Knapp 1984), which are sensitive to motions faster than 100 ps and 100 ns, respectively, give the same $T_c$ value of 180 K for myoglobin, the barrier height distribution for the structural relaxation is centred at 170 K, reflecting processes occurring in about 45 min. Comparing motions which differ 13 orders of magnitude in time yield a shift of the characteristic temperature of only 10 K. Moreover, as shown in Ostermann et al. (2000) by X-ray structure analysis, conformational changes of a myoglobin molecule occur only above $T_c$. From these facts we conclude that the dynamical transition has a functional property.

## Conclusions

H64V-Metmyoglobin shows a temperature-dependent change of ligation above 170 K. At lower temperatures, the protein and its solvent shell are structurally arrested. The ligation equilibrium is only reached if protein-specific motions soften the molecule. A typical measure for the inset of the protein-specific motions is the dynamical transition temperature. Looking on the Gaussian barrier height distribution of native myoglobin, which describes the structural relaxation, it becomes obvious why we prefer the word dynamical transition temperature instead of glass transition. The distribution is smeared out over a temperature range which seems to be too large for a glass transition. The relaxation of an intermediate in H64V, observed significantly below the dynamical transition, is an indication that the protein structure does not change and only the ligand is lost.

**Acknowledgements** We thank Dr. G.U. Nienhaus for providing the bacterial strain. This work was supported by the "Deutsche Forschungsgemeinschaft" SFB-533 and the Fonds der Chemie, and by the Russian Foundation of Basic Reseach (grant 00-15-97392 to V.E.P.).

## References

Achterhold K, Keppler C, Ostermann A, van Bürck U, Sturhahn W, Alp EE, Parak FG (2002) Vibrational dynamics of myoglobin determined by phonon assisted Mössbauer effect. Phys Rev E 65:051916

Andreani C, Filabozzi A, Menzinger F, Desideri A, Deriu A, Di Cola D (1995) Dynamics of hydrogen atoms in superoxide dismutase by quasielastic neutron scattering. Biophys J 68:2519–2523

Ansari A, Berendzen J, Braunstein D, Cowen BR, Frauenfelder H, Hong MK, Iben IET, Johnson JB, Ormos P, Sauke TB, Scholl R, Schulte A, Steinbach PJ, Wittitow J, Young RD (1987) Rebinding and relaxation in the myoglobin pocket. Biophys Chem 26:337–355

Austin RH, Beeson KW, Eisenstein L, Frauenfelder H, Gunsalus IC (1975) Dynamics of ligand binding to myoglobin. Biochemistry 14:5355–5373

Bailey S (1994) The CCP4 suite: programs for protein crystallography. Acta Crystallogr Sect D 50:760–763

Bill E, Gismelseed A, Larooque D, Trautwein AX, Nasri H, Fischer J, Weiss R (1988) Mössbauer and X-ray investigation of model compounds for the P460 center of hydroxylamine oxidoreductase from nitrosomonas. Hyperfine Interact 42:881–884

Bizzarri AR, Iakovleva OA, Parak F (1995) Spin lattice relaxation in Mössbauer spectra of metmyoglobin: investigation of crystals, water and water-glycerol solutions. Chem Phys 191:185–194

Bominaar EL, Ding XQ, Gismelseed A, Bill E, Winkler H, Trautwein AX, Nasri H, Fischer J, Weiss R (1992) Structural, Mössbauer, and EPR investigations on two oxidation states of a five-coordinate, high-spin synthetic heme. Quantitative interpretation of zero-field parameters and large quadrupole splitting. Inorg Chem 31:1845–1854

Brünger AT (1992) Free *R* value: a novel statistical quantity for assessing the accuracy of crystal structures. Nature 355:472–475
Brunori M (2001) Nitric oxide, cytochrome-*c* oxidase and myoglobin. Trends Biochem Sci 26:21–23
Carugo O (1999) Correlation between occupancy and *B* factor of water molecules in protein crystal structures. Protein Eng 12:1021–1024
Chong S-H, Joti Y, Kidera A, Go N, Ostermann A, Gassmann A, Parak FG (2001) Dynamical transition of myoglobin in a crystal: comparative studies of X-ray crystallography and Mössbauer spectroscopy. Eur Biophys J 30:319–329
Chu K, Vojtchovsky J, McMahon BH, Sweet RM, Berendzen J, Schlichting I (2000) Structure of a ligand-binding intermediate in wild-type carbonmonoxy myoglobin. Nature 403:921–923
Daniel RM, Finney JL, Smith JC (2003) The dynamical transitions in proteins may have a simple explanation. Faraday Discuss, Web, 4 July 2002
Dilg AWE, Grantner K, Iakovleva O, Parak FG, Babini E, Bertini I, Capozzi FL C, Meyer-Klauke W (2002) Dynamics of wild-type HiPIPs: a Cys77Ser mutant and a partly unfolded HiPIP. J Biol Inorg Chem 7:691–703
Doster W, Cusack S, Petry W (1989) Dynamical transition of myoglobin revealed by inelastic neutron scattering. Nature 337:754–756
Engler N, Ostermann A, Gassmann A, Lamb DC, Prusakov VE, Schott J, Schweitzer-Stenner R, Parak FG (2000) Protein dynamics in an intermediate state of myoglobin: optical absorption, resonance Raman spectroscopy, and X-ray structure analysis. Biophys J 78:2081–2092
Frauenfelder H, Parak F, Young RD (1988) Conformational substates in proteins. Annu Rev Biophys Biophys Chem 17:451–479
Frauenfelder H, Wolynes PG, Austin RH (1999) Biological physics. Rev Mod Phys 71:S419–S430
Frauenfelder H, McMahon BH, Austin RH, Chu K, Groves JT (2001) The role of structure, energy landscape, dynamics, and allostery in the enzymatic function of myoglobin. Proc Natl Acad Sci USA 98:2370–2374
Gamblin SJ, Rodgers DW (1993) In: Some practical details of data collection at 100 K. Proceedings of the CCP4 study weekend. Daresbury Laboratory, Warrington, UK
Hodel A, Kim S-H, Brünger AT (1992) Model bias in macromolecular crystal structures. Acta Crystallogr Sect A 48:851–858
Kachalova GS, Popov AN, Bartunik HD (1999) A steric mechanism for inhibition of CO binding to heme proteins. Science 284:473–476
Keller H, Debrunner PG (1980) Evidence for conformational and diffusional mean square displacements in frozen aqueous solution of oxymyoglobin. Phys Rev Lett 45:68–71
Lamb DC, Ostermann A, Prusakov VE, Parak FG (1998) From metmyoglobin to deoxy myoglobin: relaxations of an intermediate state. Eur Biophys J 27:113–125
Makinen MW, Churg AK (1983) Structural and analytical aspects of the electronic spectra of hemeproteins. In: Lever AB, Gray HB (eds) Iron porphyrins, part one. Addison-Wesley, New York, pp
Mandon D, Ott-Woelfel F, Fischer J, Weiss R, Bill E, Trautwein AX (1990) Structure and spectroscopic properties of five-coordinate (2-methylimidazolato)- and six-coordinate (imidazole)(imidazolato)iron(II) ''picket-fence'' porphyrins. Inorg Chem 29:2442–2447
Melchers B, Knapp EW, Parak F, Cordone L, Cupane A, Leone M (1996) Structual fluctuations of myoglobin from normal-modes, Mössbauer, Raman, and absorption spectroscopy. Biophys J 70:2092–2099
Morikis D, Champion PM, Springer BA, Egeberg KD, Sligar SG (1990) Resonance Raman studies of iron spin and axial coordination in distal pocket mutants of ferric myoglobin. J Biol Chem 265:12143–12145
Olson JS, Phillips GN Jr (1997) Myoglobin discriminates between $O_2$, NO and CO by electrostatic interactions with the bound ligand. J Biol Inorg Chem 2:544–552
Ostermann A, Waschipky R, Parak FG, Nienhaus GU (2000) Ligand binding and conformational motions in myoglobin. Nature 404:205–208
Parak F, Formanek H (1971) Untersuchung des Schwingungsanteils und des Kristallgitterfehleranteils des Temperaturfaktors in Myoglobin durch Vergleich von Mössbauerabsorptionsmessungen mit Röntgenstrukturdaten. Acta Crystallogr Sect A 27:573–578
Parak F, Knapp EW (1984) A consistent picture of protein dynamics. Proc Natl Acad Sci USA 81:7088–7092
Parak F, Prusakov VE (1994) Relaxation of non-equilibrium states of myoglobin studied by Mössbauer spectroscopy. Hyperfine Interact 91:885–890
Parak F, Frolov EN, Kononenko AA, Mössbauer RL, Gol'danskii VI, Rubin AB (1980) Evidence for a correlation between photoinduced electron transfer and dynamic properties of the chromatophore membranes from *Rhodospirillum rubrum*. FEBS Lett 117:368–372
Parak F, Frolov EN, Mössbauer RL, Gol'danskii VI (1981) Dynamics of metmyoglobin crystals investigated by nuclear gamma resonance absorption. J Mol Biol 145:825–833
Parak F, Knapp EW, Kucheida D (1982) Protein dynamics. Mössbauer spectroscopy on deoxymyoglobin crystals. J Mol Biol 161:177–194
Perutz MF (1979) Regulation of the oxygen affinity of hemoglobin: influence of the structure of globin on the heme iron. Annu Rev Biochem 48:327–386
Phillips SEV (1980) Structure and refinement of oxymyoglobin at 1.6 Å resolution. J Mol Biol 142:531–554
Phillips SEV, Schoenborn BP (1981) Neutron diffraction reveals oxygen-histidine hydrogen bond in oxymyolobin. Nature 292:81–82
Prusakov VE, Steyer J, Parak FG (1995) Mössbauer spectroscopy on nonequilibrium states of myoglobin: a study of r-t relaxation. Biophys J 68:2524–2530
Prusakov VE, Lamb DC, Parak F, Goldanskii VI (1999) Photoinitiated generation of reduced myoglobin intermediates at cryogenic temperatures and their relaxation. Chem Phys Rep 18:835–853
Quillin ML, Arduini RM, Olson JS, Phillips GN Jr (1993) High-resolution crystal structures of distal histidine mutants of sperm whale myoglobin. J Mol Biol 234:140–155
Read RJ (1986) Improved Fourier coefficients for maps using phases from partial structures with errors. Acta Cryst A42:140–149
Reat V, Parzelt H, Ferrand M, Pfister C, Oesterhelt D, Zaccai G (1998) Dynamics of different functional parts of bacteriorhodopsin: H-$^2$H labeling and neutron scattering. Proc Natl Acad Sci USA 95:4970–4975
Schappacher M, Ricard L, Weiss R, Montiel-Montoya R, Gonser U, Bill E, Trautwein A (1983) Synthesis and spectroscopic properties of a five coordinate tetrafluorophenylthiolato iron II ''picket fence'' porphyrin complex and its carbonyl and dioxygen adducts: analogs for the active site of cytochromes P-450. Inorg Chim Acta 78:L9–L12
Shibata Yu, Kurita A, Kushida T (1998) Real-time observation of conformational fluctuations in Zn-substituted myoglobin by time-resolved transient hole-burning spectroscopy. Biophys J 75:521–527
Silver J, Lukas B, Al-Jaff G (1984) Mössbauer studies on protoporphyrin IX iron(II) frozen solutions containing ligand that cause the iron to be a five coordinate high spin iron(II) environment. Inorg Chim Acta 91:125–128
Singh GP, Parak F, Hunklinger S, Dransfeld K (1981) Role of adsorbed water in the dynamics of metmyoglobin. Phys Rev Lett 47:685–688
Springer BA, Sligar SG (1987) High-level expressions of sperm whale myoglobin in *Escherichia coli*. Proc Natl Acad Sci USA 84:8961–8965
Steinbach PJ, Ansari A, Berendzen J, Braunstein D, Chu K, Cowen BR, Ehrenstein D, Frauenfelder H, Johnson JB, Lamb DC, Mourant JR, Nienhaus GUl, Ormos P, Philipp R, Xie A,

Young RD (1991) Ligand binding to heme proteins: connection between dynamics and function. Biochemistry 30:3988–4001

Tada T, Watanabe Y, Matsuoka A, Ikeda-Saito M, Imai K, Ni-hei Y, Shikama K (1998) African elephant myoglobin with an unusual autooxidation behavior: comparison with the H64Q mutant of sperm whale myoglobin. Biochim Biophys Acta 1387:165–176

Takano T (1977a) Structure of myoglobin refined at 2.0 Å resolution. II. Structure of deoxymyoglobin from sperm whale. J Mol Biol 110:569–584

Takano T (1977b) Structure of myoglobin refined at 2.0 Å resolution. I. Crystallographic refinement of metmyoglobin from sperm whale. J Mol Biol 110:537–568

Teng TY (1990) Mounting of crystals for macromolecular crystallography in a free standing thin film. J Appl Crystallogr 23:387–391

Thomanek UF, Parak F, Formanek S, Kalvius GM (1977) Mössbauer and susceptibility experiments on different compounds of $Fe^{3+}$-myoglobin. Biophys Struct Mechanism 3:207–227

Tilton RF, Kuntz ID, Petsko GA (1984) Cavities in proteins: structure of a metmyoglobin-xenon complex solved to 1.9 Å. Biochemistry 23:2849–2857

Vojtechovsky J, Chu K, Berendzen J, Sweet RM, Schlichting I (1999) Crystal structures of myoglobin-ligand complexes at near-atomic resolution. Biophys J 77:2153–2174

Zollfrank J, Friedrich J (1990) Spectral diffusion and thermal recovery of spectral holes burnt into a phthalocyanine doped Shpol'skii system. J Chem Phys 93:8586–8590